Statistical Study of the Effect of Particle Properties on the Particle Penetration in the Idealized Trachea

R. Piemjaiswang and B. Chalermsinsuwan

***Abstract*—The particulate matter (PM) is one of the harmful pollutants that causing an impact on human health. To study the significance of those small particle properties, the research had been conducted using three-dimensional computational fluid dynamics with the Eulerian-Lagrangian approach. The trajectories of the particles were tracked and recorded. The effect of particle diameter, particle density, and particle sphericity on the escaped particle percentage was investigated and characterized using the statistical analysis of variance. The results showed that the particle diameter, particle density, their interaction, and the quadratic effect of the particle diameter played important roles in the penetration of those injected particles.**

***Index Terms*—CFD, idealized trachea, particulate matter.**

I. Introduction

The air pollution situation arises the awareness of citizens living in a particular area where the risk of exposure to the dirty air is high [1]. The main contents of air pollution are the small particulate matter which its size is in submicron [2], [3]. Many researchers have been studied for the control and prevention of these particulate matters [4], [5]. The vulnerable groups to this adverse health impact are the children and persons with an underlying health issue [6]. To understand the factor affecting the transportation characteristic of these particles, therefore, the study of the particle penetration within the human lower respiratory system was conducted.

The difficulty for the researcher to investigate this system is the complicated geometry of the human respiratory tract in both shape and size. The measurement of the flow inside the tract is also limited which leads to the development of the idealized, simplified presentation of the human trachea as proposed by Weibel *et al*. [7] The model is symmetry and the dimension of each branch is constant with gradually reduces in diameter as the branch is expanding further from its first generation. This idealized model is widely used among the researches to investigate the flow-related behavior within the trachea in both in-vivo and numerical simulations.

This study developed the mathematical model to investigate the flow behavior of the particles using reconstructed Weibei's idealized trachea model. The statistical analysis was conducted using the three-level (3^k) factorial experimental design method to identify the significant factors affecting the deposition of the particles. The multiphase Eulerian-Lagrangian approach was used to track the particle movement within the region. The outcome of the study could give a better understanding of the particle transport and could use to identify the significant characteristic of the particulate matter in order to prevent or reduce the risk of exposure to these tiny particulate matters.

Manuscript received January 30, 2020; revised September 4, 2020. This work was supported in part by the Grants for Development of New Faculty Staff and the Grant for Research (CU-GR_62_34_23_11) from Ratchadaphiseksomphot Endowment Fund of Chulalongkorn University.

R. Piemjaiswang is with Environmental Research Institute, Chulalongkorn University, Bangkok 10330, Thailand (e-mail: ratchanon.p@chula.ac.th).

B. Chalermsinsuwan is with Department of Chemical Technology, Faculty of Science, Chulalongkorn University, Bangkok 10330, Thailand (e-mail: benjapon.c@chula.ac.th).

II. Method

A. Computational Model

The Eulerian-Lagrangian approach was used to determine the particle trajectory of individual particles fed into the considering domain. The Weibel idealized model was reconstructed from the first generation 0 (G0) to generation 4 (G4) in this study. The model reconstruction was scripted using ANSYS Design-modeler software as shown in Fig. 1. The idealized trachea model had one main inlet which then separated into two branches at the end of each generation tract. In the last generation 4, the model had sixteen outlets. The detail parameter of each generation was described in Table I.

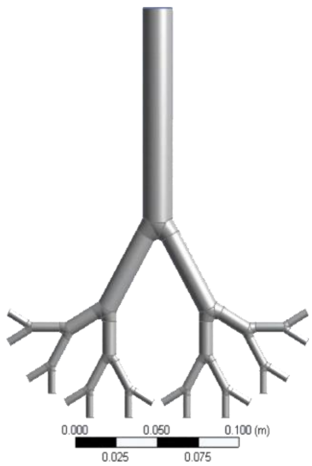

Fig. 1. Idealized trachea model.

TABLE I: The Weibel Symmetrical Model Parameters

Generation	Diameter (mm)	Length (mm)
G0	**18.0**	**120.0**
G1	12.2	47.6
G2	8.3	19.0
G3	5.6	17.6
G4	4.5	12.7

The reconstructed idealized trachea was meshed using ANSYS Mesher. The number of cells was classified with the

doi: 10.18178/ijesd.2020.11.10.1293

number of elements in the range of 150,000-400,000 elements. To ensure the accuracy of the results of the selected mesh, the mesh independence test was primarily conducted before using in the analysis.

The particle behavior at the wall of the trachea was set to collect all the particles in contact with the wall, in order to measure the amount of deposited particle. At the outlet, the particle was also collected. The collected particles at outlet implied that the particle could not reach its fate of deposition and was able to penetrate further into the deeper part of the trachea. The governing equations, including the conservation of mass and momentum, were discretized for the main flow. The model was solved for the transient solution until the flow reached the complete inhalation state. The convergence criterion of the residual was set to be less than 10^{-4}. The primary fluid flow was air, which was set as the Newtonian fluid. The model was solved using commercial finite volume solver, ANSYS CFX. The calculation was done in the 64-bit parallelized machine for the precision of the micro-scale computation. The employed governing equations are expressed as follows:

Continuity equation

$$\frac{\partial \rho}{\partial t} + \nabla \cdot (\rho \vec{u}) = 0 \tag{1}$$

Momentum equation

$$\frac{\partial \rho \vec{u}}{\partial t} + \nabla \cdot (\rho \vec{u}\vec{u}) = -\nabla p + \nabla \cdot (\bar{\bar{\tau}}) + \rho \vec{g} \tag{2}$$

$$\bar{\bar{\tau}} = \mu \left[\left(\nabla \vec{v} + \nabla \vec{v}^{T} \right) - \frac{2}{3} \nabla \cdot \vec{v} \bar{\bar{I}} \right] \tag{3}$$

The nomenclature of each symbol can be found in the CFX solver theory guide [8]. The solid particle in this study was in submicron-sized, thus, the Brownian motion could be neglected [9], [10].

B. Particle Transport Theory

Instead of being an additional phase in the Eulerian model, the solid particles in the system were being tracked as the Lagrangian approach from the beginning where the particles were fed until it trapped by the wall or escaped out of the outlet. Each particle had its own set of ordinary differential equations, including its position, velocity and mass. The injected solid particles interacted and coupled with the main flow as the source terms in mass and momentum equations. The displacement of the solid particle was computed using forward Euler integration of the particle velocity.

$$x_p^n = x_p^o + u_p^0 \delta t \tag{4}$$

$$\left(\frac{dx_p}{dt} \right) = u_p \tag{5}$$

where, u_p^0 is the initial particle velocity, *x* is the position of the tracked particle and δt is the time step. The subscript *p* referred to the particle variable. The superscript *o* and *n* are referred to old and new values, respectively. The forward integration of the aerosol particle was calculated at the end of the time step, the new particle velocity was determined using the particle momentum equation as given:

$$m_p \left(\frac{du_p}{dt} \right) = \sum F \tag{6}$$

where $\sum F$ is the summation of the forces acting on the particle. The particles discretely traveled in a continuous fluid medium, in which the acceleration of the velocity was affecting by the summation of forces. Therefore, Eq. (6) can be expanded as:

$$m_p \left(\frac{du_p}{dt} \right) = F_D (u - u_p) + F_g \tag{7}$$

In this study, only two forces are included in the model. F_D and F_g are the particle drag force and the force due to gravity, respectively. u is the fluid velocity, u_p is the particle velocity and m_p is the mass of the particle.

The drag force per unit particle mass is expressed as:

$$F_D = \frac{18\mu}{\rho_p d_p^2} \frac{C_d \operatorname{Re}_r}{24} \tag{8}$$

where μ is the dynamic viscosity of the fluid, ρ_p is the density of the particle, d_p is the particle diameter and C_d is the drag coefficient. The relative Reynolds number (Re_r) is defined as:

$$\operatorname{Re}_r = \frac{\rho d_p \left| u_p - u \right|}{\mu} \tag{9}$$

Drag force between the particles and the fluid was governed by the Schiller Naumann drag coefficient model described as:

$$C_d = \frac{24}{\operatorname{Re}_r} \left(1 + 0.15 \operatorname{Re}_r^{0.687} \right) \tag{10}$$

The sphericity (Ψ) calculation was used to interpret the particle shape into the model which refers to the ratio of the surface area of the sphere to the surface area of the particle. It is defined as:

$$\psi = \frac{\pi^{\frac{1}{3}} (6V_p)^{\frac{2}{3}}}{A_p} \tag{11}$$

where V_p is the volume of the aerosol particle and A_p is the surface area of the particle.

III. Boundary Conditions

At the inlet of the trachea, the air and the particle were fed together at the same time with the given velocity profile as sinusoidal function expressed as:

$$v = \frac{Q}{A}\sin(2\pi ft) \tag{12}$$

where Q is the volumetric flow rate, A is the cross-sectional area, f is breathing frequency and t is current flow time.

The typical average human breath with a flow rate of 30 L/min was chosen for the study. The frequency of breathing was set as the typical adult rate of 15 breaths per minute. Those fine particles were injected into the system with the rate of 10 micrograms per cubic meter of airflow. According to the United States Environmental Protection Agency (EPA) [11], the level of these harmful particles was considered in the good range which represented the best-case scenario of exposing the air pollutants. The injected particle interacted with the trachea wall by the particle-wall model. The restitution coefficient was introduced to describe the behavior of the collided particle at the wall. Normally, the wall of the trachea was not stiffed. The trachea wall was covered with the mucus-layer which was moistened and flexible. The assumption had been made that all the particles that collided with the wall will be collected on that local site. The tracking of that particular particle will be terminated. The restitution coefficient in parallel and perpendicular direction was set as zero to stop the motion of the solid particle mathematically.

At the end of the tract, the flow and the particle will reach the outlet which was assumed to have an average value of the pleural pressure. The given pressure was lower than the atmospheric pressure as it is the driving force to drive the flow of air into the lung in the inhalation phase. The particle that able to flow out from this boundary will eventually stop being tracked. The escaped solid particles flew out from the outlet were collected for their mass accumulation to further statistical analysis.

IV. Statistical Analysis

The particle properties, including particle size, particle density, and particle shape were the studied parameters. These factors were coded as A, B and C, respectively. To evaluate the significant effect of these parameters, the three-level (3^k) factorial experimental design method was used to design the set of experiments. The results were then analyzed with the statistical analysis of variance method to observe their main, interaction and quadratic effects. It is noted that the aerosol shape was not directly assigned to the variable in the equation but instead was represented as the sphericity of the particle.

Table II shows all the study factors with their coded symbol, unit and levels. The factor levels were shown in coded symbol, 1, 0 and -1, representing high level, medium level and low level, respectively. The set of experiments from the experimental design method were given in the total number of 27 trials as the technique was interpreted the parameter level with all of its combinations in order to capture their interaction effects. The value representing each level was selected from the recognized air pollutant, including PM10, PM2.5 and PM1. The density range was broadly chosen to represent the sources of the dust commonly found in the environment. The particle shape was assumed to be in a perfect sphere ($\Psi = 1$) down to 0.5.

The particle escaped percentage (ESP) is defined as:

$$ESP = \frac{\text{Total mass of particle escaped}}{\text{Total mass injected}} \times 100 \tag{13}$$

By using the indicator, high ESP would suggest that the particles can penetrate deeper into the further generation of the respiratory tree. It is noted that the complement of the ESP is not always equal to 1. This implies that not all the solid particle is deposited to the wall. Sometimes, the particles can be suspended along the tract at the end of the inhalation phase.

TABLE II: Input Parameters Considered in this Study

Coded Factor	Factor	Unit	Level		
			-1	0	1
A	Particle diameter	μm	1	2.5	10
B	Particle density	kg/m^3	900	1,775	2,650
C	Particle sphericity	-	0.50	0.75	1.00

V. Result and Discussion

A. Mesh Independence Test

The mesh independence test was conducted on the meshed trachea geometry (as shown in Fig. 1). The pressure profiles calculated from those meshes are depicted in Fig. 2. The pressure profile was plotted with the distance from the inlet. The plot shows that the results converged onto the mesh-independent state as the number of mesh elements increased. The mesh with 300,000 and 450,000 elements showed promising results distinct from the result from 150,000 elements with sufficient resolution to represent the accurate result. To optimize the computational resources and calculation time, the final converged mesh of 300,000 elements was selected for the further study.

B. Model Validation

Apart from the mesh accuracy, the model correctness was also validated. The converged results at the end of the calculation were compared against the study of Shuai *et al* [12]. The flow properties were adjusted to match with the condition reported in their experiment. The average Reynolds number in each trachea generation was compared. The results are depicted in Fig. 3. The results acquired from the model gave an adequate prediction of the Reynolds number. The minor diverse comparison was only 0.079 percent in the early generation of the trachea.

C. Preliminary Result

At the beginning stage of the inhalation, the particle had not yet been injected into the system. The flow clearly showed that the flow profile was moving faster in the middle of the tract. As the particles had got injected, some of them were trapped by the wall. The particles reached the outlet at the time of 0.4 seconds and were able to escape from the computation domain. This implied the possibility that these small particles could potentially travel deeper down to the next region of the respiratory tree.

Table III reports the total mass and percentage of the escaped aerosol for all of the cases. In case 13, 17 and 25, the result showed that the highest total mass escaped from the calculation domain with the accumulated mass of 2.1305E-11 kg. It is 63.77 percent of the total particle injected. In contrast, case 1, 5 and 10 gave the lowest total of the total mass escaped from the calculation domain with a value of 1.3355E-11 kg. The result is 39.98 percent of the total particle injected. For all these three cases for each group, they share the same settings except for the particle sphericity. The sphericity or the shape of the particle seemed not to play the roles to the particle flow especially in this size of the particle. The main difference between the maximum and the minimum cases was the particle diameter and particle density. The maximum total mass escaped was found in the cases with small particle size and low particle density. To interpret the result statistically, the analysis of variance (ANOVA) was introduced to evaluate the significance of the factors.

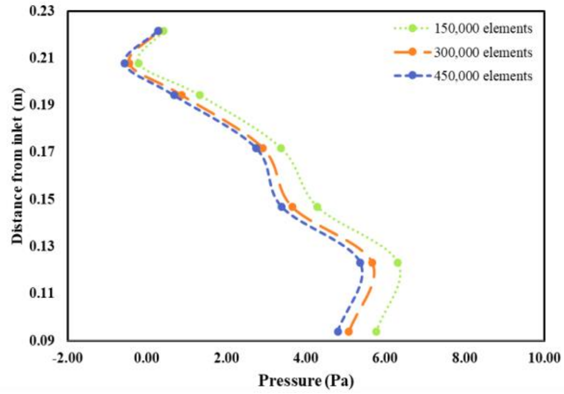

Fig. 2. Mesh independence test.

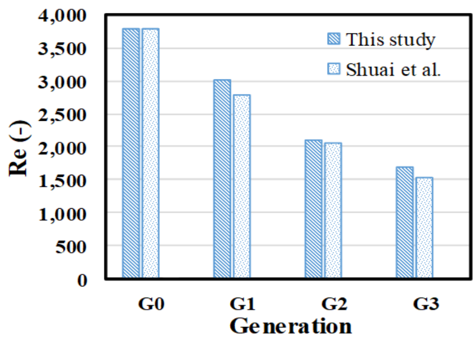

Fig. 3. Reynolds number of each generation (Q = 50 L/min).

TABLE III: THE DESIGNED EXPERIMENT WITH ALL POSSIBLE COMBINATIONS

#	Factor			Total particle escaped	
	A	B	C	(kg)	(%)
1	1	1	1	1.3355E-11	39.98
2	1	0	1	1.6705E-11	50.00
3	1	-1	-1	1.9534E-11	58.47
4	1	-1	0	1.9534E-11	58.47
5	1	1	0	1.3355E-11	39.98
6	-1	1	1	2.1282E-11	63.70
7	1	0	0	1.6705E-11	50.00
8	0	1	1	2.1069E-11	63.07
9	-1	0	0	2.1292E-11	63.73
10	1	1	-1	1.3355E-11	39.98
11	0	0	-1	2.1180E-11	63.40
12	0	0	1	2.1180E-11	63.40
13	-1	-1	-1	2.1305E-11	63.77
14	-1	1	-1	2.1282E-11	63.70
15	-1	1	0	2.1282E-11	63.70
16	0	-1	-1	2.1241E-11	63.58
17	-1	-1	1	2.1305E-11	63.77
18	0	0	0	2.1180E-11	63.40
19	1	-1	1	1.9534E-11	58.47
20	-1	0	1	2.1292E-11	63.73
21	1	0	-1	1.6705E-11	50.00
22	-1	0	-1	2.1292E-11	63.73
23	0	1	-1	2.1069E-11	63.07
24	0	-1	1	2.1241E-11	63.58
25	-1	-1	0	2.1305E-11	63.77
26	0	-1	0	2.1241E-11	63.58
27	0	1	0	2.1069E-11	63.07

D. Escaped Particle Percentage

The ANOVA was utilized to determine the significant levels of the study factors, including the particle diameter, particle density and particle sphericity. The analysis results are shown in Table IV. With the confidence interval of 95.00%, the significant factors are showing the p-value less than 0.05. The analysis results were given that the particle diameter (A), particle density (B), the interaction between particle diameter and particle density (AB), and the quadratic effect of the particle diameter (A^2) were the significant factors.

TABLE IV: ANALYSIS OF VARIANCE FOR THE PARTICLE ESCAPED PERCENTAGE

Source	SS	Df	MS	F-value	p-value
Model	1623.26	9	180.36	39.49	< 0.0001
A	913.78	1	913.78	200.06	< 0.0001
B	181.83	1	181.83	39.81	< 0.0001
C	0.0000	1	0.0000	0.0000	1.0000
AB	254.47	1	254.47	55.71	< 0.0001
AC	0.0000	1	0.0000	0.0000	1.0000
BC	0.0000	1	0.0000	0.0000	1.0000
A^2	272.70	1	272.70	59.70	< 0.0001
B^2	0.4760	1	0.4760	0.1042	0.7508
C^2	0.0000	1	0.0000	0.0000	1.0000
Residual	77.65	17	4.57		
Total	1700.91	26			

SS: Sum of squares, Df: Degree of freedom, MS: Mean square

Fig. 4 shows the surface plot of the particle escaped percentage between the particle diameter (A) and particle density (B). Within the study range, the escaped particle was low when both diameter and density was high. This is related to gravity force as the high diameter (high volumes) and high density results in higher gravity force pulling those particles. However, the particles are not able to penetrate through the outlet at the fourth generation, but they have more chance to collide to the wall instead.

Fig. 5 shows the interaction effect plot of the particle diameter and particle density (AB). The relationship between particle diameter and particle density was dependent. With the low level of particle density (B-), the particle escaped percentage showed an adverse relationship with the particle diameter. However, with the high level of particle density (B+), the inverse relationship was found. The plot showed a positive effect when the particle diameter was below the medium level (0) and showed a negative effect when the particle diameter was higher than the medium level (0).

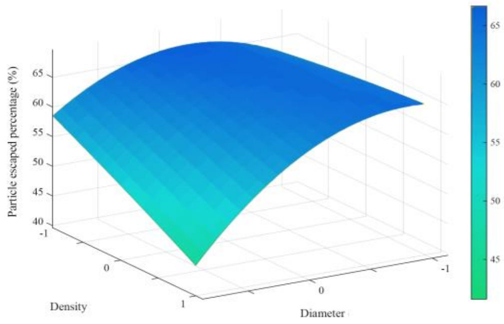

Fig. 4. The surface plot of particle escaped percentage.

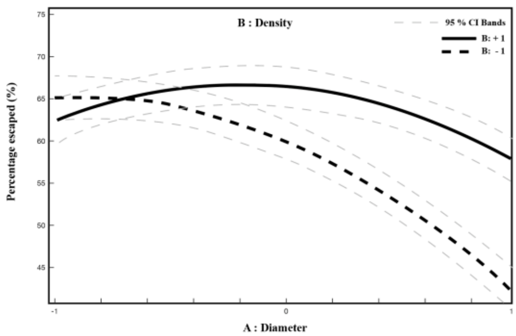

Fig. 5. The interaction plot between factor A and B.

VI. Conclusion

The upper generation 0 to 4 Weibel's idealized trachea was reconstructed and used for the three-dimensional computational fluid dynamics analysis with the Euler-Lagrangian approach. The particle transport theory was employed to track the particle trajectory using commercial ANSYS CFX solver. The mesh using in the study was verified for its mesh dependence state. The model was validated against the experimental result from Shuai *et al* [12]. The results given by the model was statistically analyst for the significance of the particle properties on the penetration of particle deep down the respiratory tree, including, particle diameter, particle density and particle sphericity. The analysis results can be concluded as:

- Aerosol diameter (A), aerosol density (B), their interaction (AB) and the quadratic effect of the aerosol diameter (A^2) were the significant factors affecting the particle escaped percentage.
- Aerosol diameter had a negative effect on the particle escaped percentage. Smaller particles penetrated deeper causing it to escape more than the particle with a large diameter.
- Aerosol density had a negative effect on the particle escaped percentage. The heavy particles collide more on the upper part of the trachea, in contrast, the light particles can travel further down the tree.
- Within the range of study, the particle escaped percentage was lowest when both particle diameter and particle density were high.

Conflict of Interest

The authors declare no conflict of interest.

Author Contributions

All authors conducted the research; analyzed the data; wrote the paper; had approved the final version.

Acknowledgment

This research was funded by Grants for Development of New Faculty Staff and the Grant for Research (CU-GR_62_34_23_11) from Ratchadaphiseksomphot Endowment Fund of Chulalongkorn University.

References

[1] Team WHOO and EH, *WHO Air quality guidelines for particulate matter, ozone, nitrogen dioxide and sulfur dioxide: Global update 2005: Summary of risk assessment*. Geneva PP - Geneva: World Health Organization.

[2] L. Bai, Z. He, W. Chen, and Y. Wang, "Distribution characteristics and source analysis of metal elements in indoor PM2.5 in high-rise buildings during heating season in Northeast China," *Indoor Built Environ*, 2019.

[3] L. Bai, Z. He, C. Li, and Z. Chen, "Investigation of yearly indoor/outdoor PM2.5 levels in the perspectives of health impacts and air pollution control: Case study in Changchun, in the northeast of China," *Sustain Cities Soc*, 2019.

[4] C. Xu and L. Liu, "Personalized ventilation: One possible solution for airborne infection control in highly occupied space?" *Indoor Built Environ*, vol. 27, pp. 873-876, 2018.

[5] R. D. Meyer and G. Tan, "Use of proper orthogonal decomposition and linear stochastic estimation technique to investigate real-time detailed airflows for building ventilation," *Indoor Built Environ*, vol. 25, pp. 378-389, 2016.

[6] R. W. Atkinson, H. R. Anderson, J. Sunyer, J. Ayres, M. Baccini, J. M.Vonk, *et al.* "Acute effects of particulate air pollution on respiratory admissions: Results from APHEA 2 project," *Am J Respir Crit Care Med*, vol. 164, pp. 1860-1866, 2001.

[7] E. R.Weibel, "Chapter VI - geometry and dimensions of airways of the respiratory zone," in *Weibel ERBT-M of the HL*, Academic Press, 1963, pp. 56-73.

[8] Ansys CFX. ANSYS CFX-solver theory guide. ANSYS CFX Release 15317, 724-746, 2009.

[9] Y. Imai, T. Miki, T. Ishikawa, T. Aoki, and T. Yamaguchi, "Deposition of micrometer particles in pulmonary airways during inhalation and breath holding," *J. Biomech*, 2012.

[10] L. T. Holbrook and P. W. Longest, "Validating CFD predictions of highly localized aerosol deposition in airway models: In vitro data and effects of surface properties," *J Aerosol Sci.*, 2013.

[11] U. States and E. Protection, *Agency. Integrated Review Plan for the National Ambient Air Quality Standards for Particulate Matter*.

[12] S. Ren, M. Cai, Y. Shi, W. Xu, and X. D. Zhang, "Influence of bronchial diameter change on the airflow dynamics based on a pressure-controlled ventilation system," *Int. J. Numer Method Biomed Eng.*, 2018.

R. Piemjaiswang is a researcher at Environmental Research Institute, Chulalongkorn University, Thailand. He received his MS and Ph.D degrees in chemical technology from Faculty of Science, Chulalongkorn University. In addition, he finished his bachelor degree of engineering in petrochemical and polymeric material from Silpakorn University, Thailand. His main research topics are focusing on the

environmental problems in applied with computational fluid dynamics (CFD). Besides, the human health related to the change of the environment is also his concerned.

B. Chalermsinsuwan is an associate professor of Department of Chemical Technology at Faculty of Science, Chulalongkorn University. He hold a B.Sc. in chemical engineering from Chulalongkorn University and Ph.D. degree in chemical technology from Chulalongkorn University. His research interest relates to the several topics include computational fluid dynamics (CFD) simulation, experimental design and analysis, multiphase flow/fluidization technology and carbon dioxide (CO_2) capture and utilization.